Accuracy of Localization of Prostate Lesions Using Manual Palpation and Ultrasound Elastography

Carmen Kut[a], Caitlin Schneider[b], Naima Carter-Monroe[a], Li-Ming Su[c], Emad Boctor[a], Russell Taylor[b]

[a]Johns Hopkins Univ. School of Medicine, Baltimore, MD 21287-0910
[b]Johns Hopkins Univ., Baltimore, MD 21218
[c]Department of Urology, Univ. of Florida College of Medicine, Gainesville, FL 32607

ABSTRACT

Purpose: To compare the accuracy of detecting tumor location and size in the prostate using both manual palpation and ultrasound elastography (UE). **Methods**: Tumors in the prostate were simulated using both synthetic and ex vivo tissue phantoms. 25 participants were asked to provide the presence, size and depth of these simulated lesions using manual palpation and UE. Ultrasound images were captured using a laparoscopic ultrasound probe, fitted with a Gore-Tetrad transducer with frequency of 7.5 MHz and a RF capture depth of 4-5 cm. A MATLAB GUI application was employed to process the RF data for ex vivo phantoms, and to generate UE images using a cross-correlation algorithm. Ultrasonix software was used to provide real time elastography during laparoscopic palpation of the synthetic phantoms. Statistical analyses were performed based on a two-tailed, student t-test with $\alpha = 0.05$. **Results:** UE displays both a higher accuracy and specificity in tumor detection (sensitivity = 84%, specificity = 74%). Tumor diameters and depths are better estimated using ultrasound elastography when compared with manual palpation. **Conclusions**: Our results indicate that UE has strong potential in assisting surgeons to intra-operatively evaluate the tumor depth and size. We have also demonstrated that ultrasound elastography can be implemented in a laparoscopic environment, in which manual palpation would not be feasible. With further work, this application can provide accurate and clinically relevant information for surgeons during prostate resection.

Keywords: Ultrasound Elastography, manual palpation, lesion localization, ultrasound phantoms

1. INTRODUCTION

1.1 Objective

This study aims to demonstrate that ultrasound elastography (UE), a new mode of ultrasound imaging, can complement manual palpation in identifying palpable lesions in solid organs such as the prostate.

1.2 Background

Manual palpation of the prostate gland has traditionally been used to determine the presence of firm lesions at the surface of the gland during surgery, to remove a cancerous prostate gland, to guide the surgeon in excising wider tissue in efforts to avoid leaving tumor behind. However, there are several challenges that physicians face in using this technique. First, surgeons today lack a comprehensive and accurate method in determining the presence and precise location of multiple lesions during prostate excision. Secondly, manual palpation often fails to detect lesions that are small or located deep within the prostate tissue, where tactile discrimination may be difficult if not impossible. Although B-mode ultrasound can assist the surgeon in examining certain types of lesions, some prostate tumors are isoechoic to the normal surrounding prostate tissue and therefore cannot be identified using this modality. Ultrasound elastography is an imaging modality that may play a role in identifying these isoechoic tumors[2].

Medical Imaging 2009: Visualization, Image-Guided Procedures, and Modeling,
edited by Michael I. Miga, Kenneth H. Wong, Proc. of SPIE Vol. 7261, 726128

Ultrasound Elastography is a non-invasive imaging method in which the elastic properties of tissues can be used to detect or classify lesions [5]. Since cancerous lesions are up to 30 times stiffer than normal soft tissues, this elastic property of human tissues can be used in UE to differentiate tumors from surrounding normal tissues [6]. By comparing the radio frequency (RF) data of prostate lesion phantoms before and after compression, strain images can be generated using cross-correlation algorithms. Stiffer lesions tend to generate lower strain values when compared to the softer surrounding tissues. Thus, this mode of imaging provides a novel view of the tissue that is otherwise not possible using the traditional B-mode ultrasound.

1.3 Specific Aims

A randomized control study was designed to compare the accuracy in detecting prostate lesions using both manual palpation and ultrasound elastography (UE). We aimed to develop realistic, reusable ultrasound phantoms for lesion detection using UE.

To facilitate the use of ultrasound elastography, our team also developed a MATLAB application which expedites UE image processing and provides a graphical user interface (GUI) for easy interaction. Using this application, surgeons can quickly obtain the data needed to make informed and accurate determinations about the size and depth of lesions.

Finally, in laparoscopic and robotic prostatectomy surgeries, a surgeon loses haptic feedback to which they are accustomed and therefore can not manually palpate the surface and substance of the prostate gland during surgery. Without haptic feedback, this may in theory result in inadequate resection of tumor-free tissue margin around a tumor located at the surface of the prostate specimen resulting in tumor recurrence. Therefore it is during these minimally invasive interventions where imaging and identification of tumors using ultrasound elastography may prove most useful. Our study aims to demonstrate the use of laparoscopic ultrasound probes in generating UE images.

2. METHODOLOGY

2.1 Phantom Design

Seven synthetic phantoms and four ex vivo (chicken) phantoms were created for the experiment. Synthetic phantoms were made from Liquid Plastic (M-F manufacturing) [1] and glass micro-beads. The micro-beads were used as a scattering material, and concentration of the beads was adjusted to mimic the acoustic properties of human tissue. Once this optimal concentration was identified, it was applied identically to both lesions and phantom; consequently, the lesions appear isoechoic under B-mode ultrasound. Several different types of liquid plastic were used, which ranges from super soft to hard. By varying the mixing ratios of the plastic types, we could create lesions that were stiffer than the surrounding phantom material.

Lesions were colored pink for easier identification. This allows the research team to obtain ground truth of the tumor size, depth and location. To prevent the test subjects from directly visualizing the simulated lesions, however, the superior surface was colored opaque blue. The phantoms were approximately three inches in length, two inches in width and two inches in depth (3 x 2 x 2 inch). Each phantom was build with any where from zero to three lesions. Phantoms without palpable lesions, which were used as a control, were still constructed with pink pseudo-tumors of the same stiffness as the main phantom. In this case, even if subjects were to inadvertently see the phantoms, they would not have been given a clue that there were no palpable lesions present. Phantoms were built to mimic the approximate size and texture of the human prostate. The phantoms were built in layers in order to specifically control both the location and depth for each lesion. Lesions were constructed and shaped separately into spheres ranging in diameter from 1.0 cm to 2.0 cm. For ex vivo phantoms, raw chicken breasts were used; lesions were simulated using radio frequency (RF) ablation. The ablation was performed at an average of 95 degrees Fahrenheit for 20 minutes. This formed a hard spherical lesion of cooked chicken. By changing the probe insertion, lesion diameter could be controlled. These lesions were created at a depth of 1-25 mm below the surface, which allowed for possible palpation but not the visual localization of lesions.

Before ablation, the chicken was placed in a small plastic container and surrounded by 150 bloom porcine gelatin. This gelatin provided support for the chicken phantom, and prevents it from subsequent degradation and desiccation. Whereas synthetic phantoms could be used throughout the study, each chicken phantom could only be stored and used for about 2 days.

Ground truth could be determined from both types of phantoms. Lesion locations were manually measured to find their diameter and depth. This could be completed quickly and accurately due to the pink color of the lesions and the transparency of the phantom. X-ray scans were used to localize ablation sites in the chicken phantoms and after the experiments had been completed the phantom was sliced and sectioned to determine the depth and extent of the ablated area.

1A. 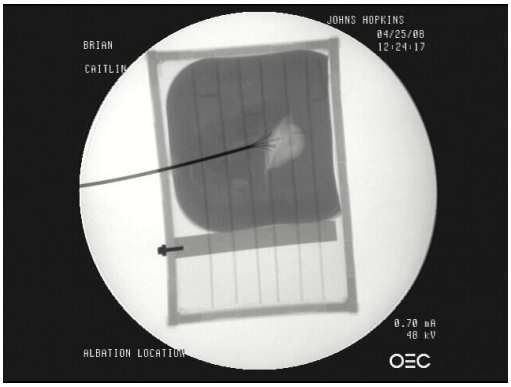

1B. 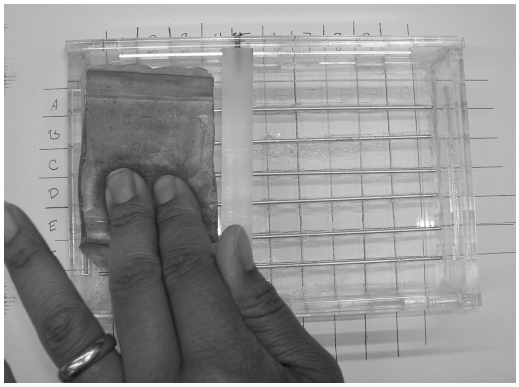

Figure 1A. X-ray of ex vivo chicken phantom. Ablation probe, tines and the grid on of the box are clearly visible.

B. Synthetic phantom, with grid box as reference

2.2 Hardware Specifications

Ultrasound images were captured using a laparoscopic ultrasound probe, fitted with a Gore-Tetrad transducer. To collect ultrasound data, we used the Ultrasonix RP Platform. Some of these capabilities include: RF Data 20 MHz @ 16 bits and RF Capture Real-time Viewing Mode. We also made use of the elastography algorithms of Ultrasonix in addition to others. The Laparoscopic ultrasound probe used during these trials had a center frequency of 7.5 MHz, and 128 elements. The ultrasound probe was placed at a fixed angle to the phantom, and one of the experimenters palpated the phantom gently in order to ensure that the probe was moved vertically in one-dimension.

2.3 Elastography Algorithms

Two methods were used to produce elastography images in this study. The first method was to use the software currently available from Ultrasonix, while the other involved the implementation of a MATLAB-based, cosine-fit cross correlation algorithm [3, 5]. For the synthetic phantoms, the Ultrasonix software was used for analysis. For the ex vivo (chicken) phantoms, the MATLAB-based algorithm was implemented.

Cross-correlation is the measure of similarity between two waveforms or images, as a function of the time lag between them. The algorithm can be simplified as follows:

$$(f \star g)[n] \stackrel{\text{def}}{=} \sum_{m=-\infty}^{\infty} f^*[m]\ g[n+m].$$

In our implementation, since the RF data can vary due to differences in conditions, we first computed displacement estimation based on a normalized cross-correlation computation. This can be accomplished by subtracting the mean and then divided the RF data by the standard deviation:

$$\frac{1}{n-1}\sum_{x,y}\frac{(f(x,y)-\overline{f})(t(x,y)-\overline{t})}{\sigma_f \sigma_t}$$

where n is the number of pixels in the RF signals t(x,y) and f(x,y). After the normalization algorithm, we then applied a cosine-fit to the data, evaluated the image similarity based on interpolation and eventually implemented the strain calculation for the ultrasound data.

To optimize the usability of our software, we have developed a MATLAB GUI Toolkit for generating elastography images. This toolkit allows for flexible manipulation of parameters, which includes search window size, window overlapping size and the predicted average strain of compressed B-mode. It also enables the user to adjust the elastography images by implementing median filters, least square algorithms and strain value thresholding.

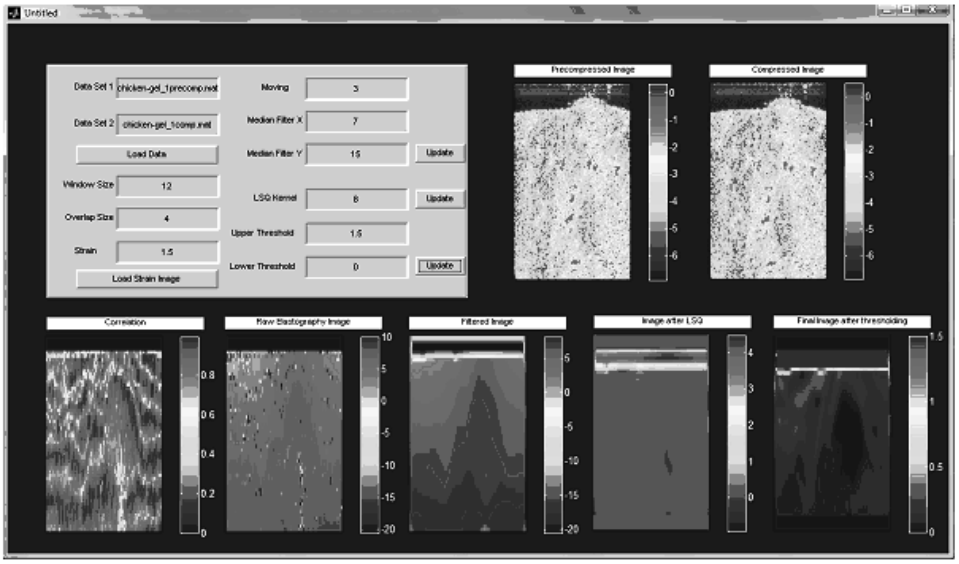

2A.

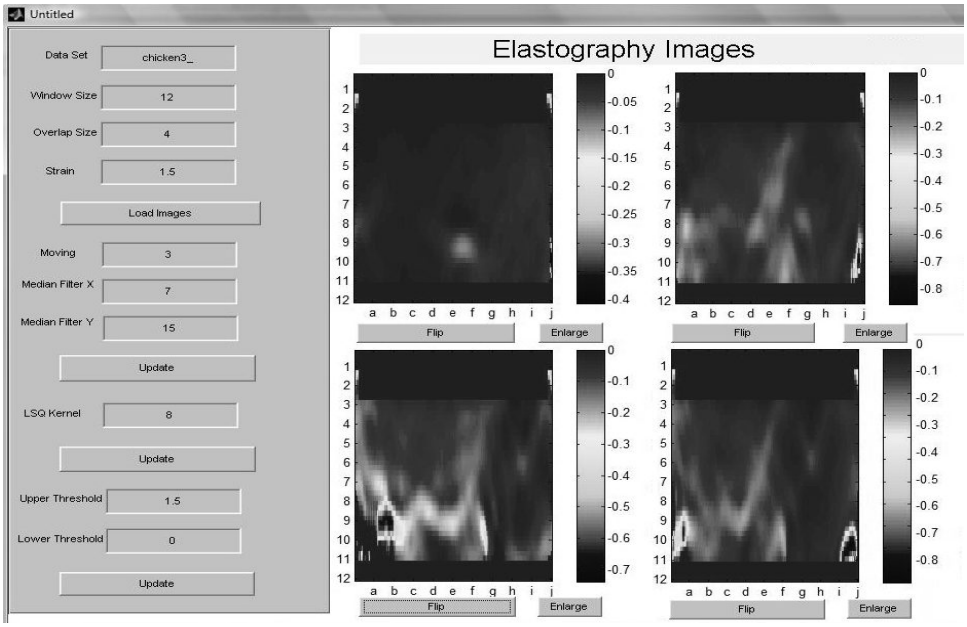

2B.

Figure 2. A-B MATLAB application, used in data analysis for ex vivo (chicken) phantoms 2A. Researcher Interface, contains correlation image, raw elastography image, filtered image and final elastography image after LSQ 2B. Participant Interface, contains final elastography images for different cross-sections of chicken phantom.

2.4 MATLAB Toolkit Design

A MATLAB GUI application was designed to process the RF data and to generate UE images using a cross-correlations algorithm. The graphical user interface (GUI) enabled participants to view all cross-sections of the phantom in a single panel. A separate scale in centimeter was also provided in determining lesion depth (in the z direction). To allow for easier viewing and analysis, participants were able to enlarge each cross-sectional image and also to view each cross-section separately.

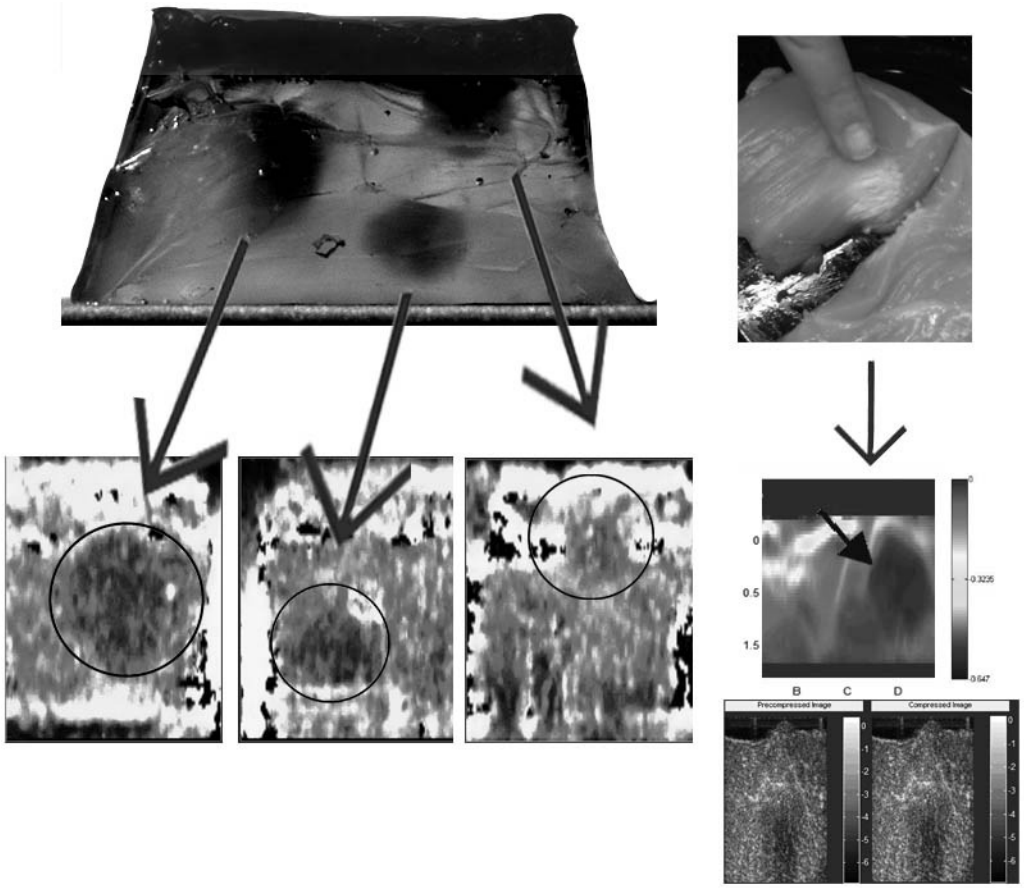

Figure 3. B-mode and elastography images. Left: synthetic phantoms with real time elastography Right: Chicken Phantoms with MATLAB cross-correlation, cosine-fit algorithm

2.5 Experimental Protocol

25 participants, recruited from local undergraduate students, graduate students and PhD-level researchers, were asked to identify lesions using both synthetic and ex vivo phantoms. In this study, each subject was asked to report lesion diameter and depth in three to four phantoms. Since most subjects had no previous ultrasound experience, all subjects underwent a training session in which they were shown sample UE images. The concept and implementation of this method were explained, and subjects were taught to identify lesions within these images. Recommended methods for manual palpation were also demonstrated and the subjects were allowed to see the ground truth for a sample phantom.

After the training session, three to four phantoms were randomly selected for the subject. Each phantom was then placed in a self-designed calibration box, which consisted of a 0.5x0.5 inch grid, labeled with numbers or letters along each axis. This grid provided the subjects with a consistent scale against which to make their measurements. Subjects were given five minutes to perform a complete search of the phantom and identify each lesion. The subjects were asked to identify each lesion with in a phantom and then estimate the lesions diameter and depth from the surface.

For initial trials with the ex vivo (chicken) phantoms, images were shown in the MATLAB application. For these ex vivo trials, subjects were presented with a series of cross sectional images of the phantom, labeled with the appropriate grid numbers and letters, which together represent images from the entire phantom. From these images, subjects were asked to provide the presence, size and depth of these simulated lesions.

For later trials completed using the synthetic phantoms, Ultrasonix software was used to obtain real time elastography images. All subjects were shown images in a red color map, where the dark areas were mapped to hard tissue and the light area represented softer tissue. This method provided the subjects with a series of images and enabled them to better filter out the noise in the image from the lesion itself. The lesions identified in the images were then measured using a ruler to determine the diameter and depth of each lesion found.

Due to the relative inexperience of our subjects, it was not possible to have the subjects create their own UE images. Thus, to maintain consistent image quality, elastography images were consistently obtained by one of our researchers.

The order in which the subjects completed the UE and manual portions of the task was randomized to prevent any learning bias. Institutional Review Board approval from the Johns Hopkins University was obtained for this study.

2.6 Statistical Analysis

Accuracy was determined descriptively using box and whiskers plots, sensitivity and specificity calculations, and calculation of the root mean squared error of estimation (RMSE) obtained from subtracting the estimated value of the measured parameter (diameter or depth) from the true value (ground truth) determined from direct observation.

STATA 9 was used to perform the statistical analysis, which consisted of Student's t-test for comparison between the means of the RMSE of both diameter and depth as estimated via manual palpation versus ultrasound. The p-values reported were generated by t-test calculations assuming unequal variances for a two-tailed test where $p = 0.05$.

3. RESULTS AND DISCUSSION

3.1 Hypothesis

Our initial hypothesis was that manual palpation is less accurate at determining lesion depth and diameter than ultrasound elastography. We also hypothesized that manual palpation has a lower overall detection rate when compared with ultrasound elastography.

3.2 Lesion Detection

The sensitivity and specificity in lesion detection were computed for both manual palpation and ultrasound elastography. Results are shown in Table 1 below. Specificity is calculated as the proportion of true positives, which are correctly identified, and the specificity is calculated as the proportion of true negatives, which are correctly identified.

Overall, ultrasound elastography displays a higher accuracy in tumor detection with a sensitivity of 84% and specificity of 71%, compared to a sensitivity of 66% and a specificity of 67% for manual palpation. While manual palpation (80%) had a higher detection rate than ultrasound elastography (68%) at a depth of < 20 mm, ultrasound elastography (66%) greatly exceeded the detection rate for manual palpation (0%) at a depth of >20 mm.

	Manual Palpation	Ultrasound Elastography
Sensitivity	66%	84%
Specificity	67%	71%
Detection rate <20 mm depth	80%	68%
Detection rate >20 mm depth	0%	66%
Detection Rate	80%	84%

Table 1. Experimental Results: Sensitivity and Specificity

3.3 Lesion Diameter

Using a Student's t-test for comparison of means, we concluded that the root mean squared error (RMSE) of diameter estimation using manual palpation is less accurate than estimations made using ultrasound elastography ($P = 0.001$) with a mean RMSE = 4.81 for manual palpation (95% CI between 3.83 and 5.78) and a mean RMSE = 3.02 for ultrasound elastography(95% CI between 2.57 and 3.47).

For ex vivo phantoms, estimations were comparable in both manual palpation and ultrasound elastography, at a RMSE of about 11.0 mm. Also, as we had a limited number of trials (4 participants) for the ex vivo phantom data, significance of results cannot be calculated.

3.4 Lesion Depth

The depth of each lesion was estimated as the distance between the surface of the phantom and the top of the lesion itself. Here, we concluded that the difference between the RMSE of depth estimation using manual palpation is statistically higher than that of ultrasound elastography ($P = 0.0001$) with a mean value of the RMSE of 8.81 for manual palpation (95% CI between 6.24 and 11.39) and a mean value of the RMSE=3.02 for ultrasound elastography(95% CI between 2.42 and 3.63). This is consistent with the findings in Figures 4A and 4B, which show higher values for the RMSE in diameter and depth estimation using manual palpation versus ultrasound elastography.

For ex vivo phantoms, participants performed well in estimating lesion depth for both manual palpation and ultrasound elastography, at a RMSE of about 1.0 mm. However, this could be an artifact, as all lesions in the ex vivo phantoms were rather superficial, and were at a depth of less than 7mm. Once again, due to the limited number of trials (4 participants), significance results could not be calculated.

3.5 Discussion

While the data from synthetic phantoms demonstrated that UE was more accurate in determining tumor diameter and depth, our data from the ex vivo phantoms showed comparable results for both manual palpation and ultrasound elastography. This could be attributable to two factors. First of all, in our trials for ex vivo phantoms, subjects were given offline, MATLAB-based elastography images instead of real time elastography. Consequently, subjects were only given a single elastography image for each cross section to examine. Because of the noise in the image, many subjects consistently identified artifacts in the image as a lesion. If the subjects were able to create images in real time, we are

confident that they would be able to filter out the noise, and find the lesion, which would be consistent from one image to the next. In contrast, in our trials for synthetic phantoms with real time elastography, participants were able to filter out the noise from the image sequences, and performed much better in localizing lesions. Secondly, the lesions in the ex vivo phantoms were rather superficial, at a depth of < 7 mm. This is in contrast to our lesions in the synthetic phantoms, which were distributed at a depth of between 7-25mm. Consequently, it was much easier to manually palpate for the lesions in the ex vivo phantoms than in the synthetic phantoms.

The number of false positives reported during the ultrasound image inspection can be contributed to the inexperience of our subjects. Ultrasound and ultrasound elastography are unfamiliar to many of our subjects, and although they did receive some training, many participants consistently identified artifacts in the image as lesions. If the subjects were able to have additional training sessions and learn to produce images themselves, we are confident that they would be able to better filter out the noise, and correctly identify the lesions. In this way, the trial was somewhat biased toward manual palpation. Manual palpation is a very intuitive and innate act for a human, where many of our subjects had never seen an ultrasound or elastography image before. With additional training time and more exposure to the types of images, it is believed that our results would improve.

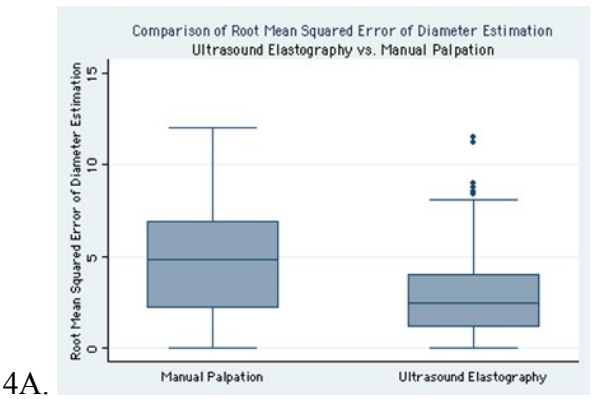

4A.

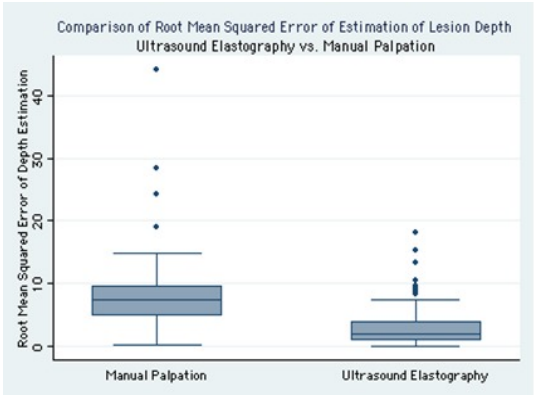

4B.

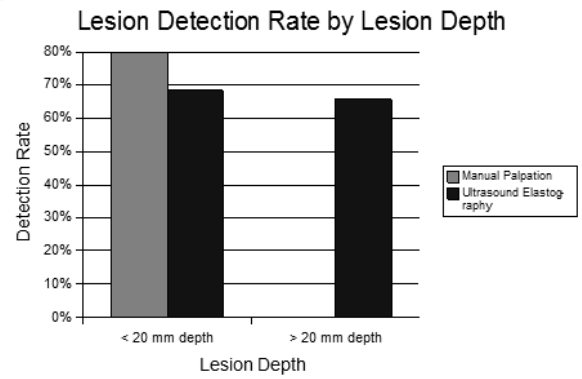

4C.

Figure 4. A-C Synthetic Phantom Results for synthetic phantoms in determining lesion diameter, depth and detection rate

4. NEW/BREAKTHROUGH WORK

Intraoperative assessment of the presence of a prostate lesion especially at the surface of the prostate gland is important in a surgeon's determination of the indication and extent of excising additional tissue in efforts to avoid leaving tumor behind. This is especially relevant in minimally invasive surgical approaches to prostatectomy such as laparoscopic or

robotic surgery where tactile feedback is no longer possible. Having a means of "palpating" the prostate through either haptic technology or imaging may serve to improve intraoperative surgical decision-making during these surgeries. To our knowledge, there has been no study that directly compares the performance of ultrasound elastography with that of manual palpation. In this work, we have demonstrated that ultrasound elastography can approach the efficacy of manual palpation in identifying prostate lesions. The present study also shows strong potential for the use of ultrasound elastography in laparoscopic surgeries. For the study, our team succeeded in developing a realistic, reusable ultrasound prostate phantom for lesion detection using UE. We have also developed a MATLAB GUI application which expedites UE image processing and provides a graphical user interface (GUI) for easy interaction.

5. CONCLUSIONS

Ultrasound elastography has strong potential in assisting surgeons to intra-operatively detect and localize lesions within the prostate gland. Our results have indicated that ultrasound elastography can produce results for lesion depth and size that are significantly better than those in manual palpation. More importantly, we have also demonstrated that ultrasound elastography can be implemented in a laparoscopic environment, where manual palpation is not feasible. We are currently in the process of obtaining an IRB for a similar study with the use of malignant prostate samples. In addition, the lower limits of lesion detection in terms of size and depth need to be further defined with UE. With further refinements, such as better hardware implementations and improved user-interface, we are confident that UE application can provide accurate and clinically relevant information for surgeons during surgical excision of the lesions such as for prostate cancer.

6. ACKNOWLEDGEMENTS

We thank our surgeon colleague Dr. Mohammed Allaf for helpful advice.

This work was supported in part by NSF ERC grant EEC 9731748 and in part by NIH Grant 2 R42 RR019159

REFERENCES

[1] DiMaio, S.P. Salcudean, S.E., "Robotics and automation," IEEE Transactions. 19(5), 864-875 (2003)

[2] Hiltawsky, K., "Freehand ultrasound elastography of breast lesions: clinical results," Ultrasound in medicine & Biology. 27(11), 1451 (2001)

[3] C´espedes,I., Y. Huang, J. Ophir, and S. Spratt, "Methods for estimation of subsample time delays of digitized echo signals," Ultrason. Imaging. 17(2), 142-171 (1995)

[4] Konofagou, Elisa E., Tim Harrigan, Jonathan Ophir, "Shear strain estimation and lesion mobility assessment in elastography," Ultrasonics. 38(1), 400-404 (2000)

[5] Bilgen, M., Insana, M.,"Deformation models and correlation analysis in elastography," J. Acoust. Soc. Am. 99 (5), (1996)

[6] Ophir, J., I. Céspedes, H. Ponnekanti, Y. Yazdi and X. Li, "Elastography: a quantitative method for imaging the elasticity of biological tissues," Ultrasonic Imaging. 13(2), 111-134 (1991)